Role of the $N^*(1535)$ in the $J/\psi \to \bar{p}\eta p$ and $J/\psi \to \bar{p}K^+\Lambda$ reactions

L. S. Geng,[1] E. Oset,[1] B. S. Zou,[2] and M. Döring[3]
[1]*Departamento de Física Teórica and IFIC, Universidad de Valencia-CSIC, E-46071 Valencia, Spain*
[2]*Institute of High Energy Physics, Chinese Academy of Sciences, P. O. Box 918(4), Beijing 100049, People's Republic of China*
[3]*Institut für Kernphysik, Forschungszentrum Jülich GmbH, D-52425 Jülich, Germany*
(Received 18 July 2008; published 13 February 2009)

We study the $J/\psi \to \bar{p}\eta p$ and $J/\psi \to \bar{p}K^+\Lambda$ reactions with a unitary chiral approach. We find that the unitary chiral approach, which generates the $N^*(1535)$ dynamically, can describe the data reasonably well, particularly the ratio of the integrated cross sections. This study provides further support for the unitary chiral description of the $N^*(1535)$. We also discuss some subtle differences between the coupling constants determined from the unitary chiral approach and those determined from phenomenological studies.

DOI: 10.1103/PhysRevC.79.025203 PACS number(s): 14.20.Gk, 12.39.Fe, 13.30.Eg, 13.75.Jz

I. INTRODUCTION

Understanding the nature of various hadrons has always been a main goal pursued in studies of strong interaction phenomena. With the advent of quantum chromodynamics (QCD) the hope was raised that one could understand the various hadrons observed in nature as quarks and gluons bound together by the strong interaction. For instance, in terms of these degrees of freedom, baryons and mesons are often seen as qqq or $q\bar{q}$ composites, respectively. There are, however, certain resonances that cannot easily fit into this picture, for instance, the $\Lambda(1405)$ and the $N^*(1535)$.

The $N^*(1535)$ with a mass higher than that of the lowest $J^P = 1/2^+$ radial excitation state $N^*(1440)$ has long been a problem in conventional quark models [1]. In recent years, a new interpretation has been proposed based on studies performed within unitary chiral theories (UχPT); i.e., it is dynamically generated from the interaction of the octet of the pseudoscalar mesons and the octet of the proton [2–5]. In these studies, its extremely strong coupling to the ηN channel [6] comes out naturally. In addition, a strong coupling of the $N^*(1535)$ to the $K\Sigma$ and $K\Lambda$ channels is predicted, the latter seems to be consistent with recent analyses of the $J/\psi \to \bar{p}K^+\Lambda$ [7,8], $pp \to pK^+\Lambda$ [9], and $\gamma p \to K^+\Lambda$ reactions [10,11]. Several further studies utilizing the UχPT amplitudes have also been performed recently [12–14], which all support the UχPT description of the $N^*(1535)$.

The J/ψ and ψ' experiments at the Beijing Electron-Positron Collider (BEPC) provide an excellent place for studying excited nucleons and hyperons [15]. In Ref. [7], based on the BES results on $J/\psi \to \bar{p}\eta p$ [16] and $J/\psi \to \bar{p}K^+\Lambda$ [17], the ratio between the effective coupling constants of the $N^*(1535)$ to $K\Lambda$ and $p\eta$ is determined to be $R = g_{N^*(1535)K\Lambda}/g_{N^*(1535)\eta p} = 1.3 \pm 0.3$. Together with the previously fixed $g_{N^*(1535)\eta p}$, they were able to reproduce recent $pp \to pK^+\Lambda$ near-threshold cross-section data [18–21] very well.

In Ref. [7], it was noted that the $g_{N^*(1535)K\Lambda}/g_{N^*(1535)\eta p}$ ratio obtained there by fitting the BES data is larger by a factor of two than the corresponding UχPT one [5]. This raises naturally the question whether the UχPT picture of the $N^*(1535)$ is consistent with the BES data and how to understand the difference in the values of the coupling constants. In the present work, we aim to answer these questions by studying the reactions $J/\psi \to \bar{p}\eta p$ and $J/\psi \to \bar{p}K^+\Lambda$ within the unitary chiral approach.

This article is organized as follows. In Sec. II, we briefly outline the unitary chiral theory and the dynamical generation of the $N^*(1535)$. In Sec. III, we lay down the formalisms to study the reactions $J/\psi \to \bar{p}\eta p$ and $J/\psi \to \bar{p}K^+\Lambda$. Results and discussions are given in Sec. IV, followed by a brief summary in Sec. V.

II. UNITARY CHIRAL THEORY AND THE DYNAMICAL GENERATION OF THE $N^*(1535)$

Unitary chiral theories start with an interaction kernel, V, provided by the corresponding chiral Lagrangians, either lowest order or higher order. In Ref. [2] the Lippmann-Schwinger equation in coupled channels was used to provide a unitary amplitude in the study of meson-baryon interaction. In Ref. [22] also the Lippmann-Schwinger equation in coupled channels was used in the case of the meson-meson interaction. Yet, as noted in Ref. [23], the method of Ref. [22], integrating explicitly the q^0 variable in the loops and using relativistic propagators, corresponds to a coupled channel Bethe Salpeter equation, and most of the recent works on the topic [4,5,24–29] adhere to this method and this nomenclature.

Other unitarization procedures are obtained using the Inverse Amplitude Method (IAM) [30–32] and the N/D method [33,34].

In the Bethe-Salpeter equation method, which we employ in the present work, one has in matrix form

$$T = (1 - VG)^{-1}V, \tag{1}$$

where T, V are complex matrices in coupled channels and G is a diagonal matrix with its element the two-body loop function. In "full form," the Bethe-Salpeter equation is an integral equation where the kernel V has the full spin and angular momentum dependence and the propagators appear in their full covariant form (see, e.g., Refs. [35,36]). In the present case, one studies only the s-wave scattering amplitude and V is already projected in s wave. In addition, in the case of meson-baryon interaction, only the positive energy part of the baryon propagator (with relativistic energies) is kept, while the relativistic propagator of the mesons is taken. As it has been demonstrated with numerous examples, one can render the complex integral equations into algebraic ones by using the on-shell approach with the argument that the off-shell components can be absorbed by redefining the corresponding coupling constants [22]. It also finds an equivalent interpretation in the N/D method that relies upon a dispersion relation for T^{-1} [33,34].

The equivalence of the N/D method and the on-shell factorized Bethe-Salpeter equation, Eq. (1), follows when using the N/D method, neglecting the left-hand cut as a source of the imaginary part in the dispersion relation (see Ref. [37] for a precise and pedagogical exposition). As described in Refs. [33] and [34], the contribution of the left-hand cut in the physical region is either very small or, in any case, very weakly energy dependent, such that its effects are easily incorporated by means of the subtraction constants of the dispersion integral. A more detailed explanation of these facts can be found in Sec. II of Ref. [38].

To study the $J/\psi \to \bar{p}\eta p$ and $J/\psi \to \bar{p}K^+\Lambda$ reactions through intermediate $N^*(1535)$ [$\bar{N}^*(1535)$], we are interested in the $S = 0$ and $Q = +1$ sector with the following six coupled channels:

$$\pi^0 p,\ \pi^+ n,\ \eta p,\ K^+\Sigma^0,\ K^+\Lambda,\ K^0\Sigma^+. \tag{2}$$

The lowest order chiral Lagrangian responsible for the meson-baryon interaction is [39]

$$\mathcal{L} = \langle \bar{B}(i\gamma^\mu D_\mu - M_B)B\rangle + \frac{D}{2}\langle \bar{B}\gamma^\mu\gamma_5[u_\mu, B]\rangle + \frac{F}{2}\langle \bar{B}\gamma^\mu\gamma_5\{u_\mu, B\}\rangle. \tag{3}$$

The term with the covariant derivative, D_μ, in this Lagrangian provides the *MMBB* transition amplitude, i.e., the Weinberg-Tomozawa interaction,

$$V_{ij} = -C_{ij}\frac{1}{4f_i f_j}\bar{u}(p')\gamma^\mu u(p)(k_\mu + k'_\mu), \tag{4}$$

with p (k), p' (k') being the initial and final momenta of the baryons (mesons). The coefficients C_{ij} can be found in Ref. [12]. The terms with the D and F couplings account for the Yukawa coupling of a single meson to baryons and will play a role, by analogy, in the posterior discussions. At low energies, the amplitudes V_{ij} can be simplified by retaining the largely dominant γ^0 component and one finds an easy analytical expression for V_{ij} [5,25]. In Eq. (4) f_i (f_j) is the meson decay constant with $f_\pi = 93$ MeV, $f_K = 1.22 f_\pi$, and $f_\eta = 1.3 f_\pi$ [5].

The use of different meson decay constants, as well as other details of the calculation in Ref. [5] require some explanations. In Ref. [5] only the lowest order meson-baryon chiral Lagrangian of Eq. (3) is used. The subtraction constants in the dispersion integral or loop function, G of Eq. (1), are assumed to account for effects of higher order Lagrangians. There is, however, a caveat in this assumption because in chiral perturbation theory the loop terms contribute to order Q^3 for the case of meson-baryon interaction (the counting is different in the meson-meson interaction), while there are chiral Lagrangians of order Q^2 that would not be accounted for by means of the subtraction constants [3,26,27,29]. The effects of using different f_i are also technically of order Q^3. Although the unitary resummation will mix different powers of Q, the aim of the chiral unitary approach is to provide a unitary framework at higher energies that matches exactly the chiral perturbation theory amplitude at low energies [34]. For the meson-baryon interaction the matching should be done at order Q^3. The ability of the method used in Ref. [5] to provide realistic amplitudes depends upon the Q^2 terms being small. This is, of course, a matter of principle. In practice, and as one is usually concerned about a relatively narrow band of energies, the subtraction constants can approximately account for these Q^2 terms. Ultimately, it is the comparison of theoretical calculations done with the lowest order Lagrangian with those including higher order terms that must tell us how accurate the lowest order can be. Such a comparison is possible now. Indeed, in Ref. [29], where higher order Lagrangians are used, an estimation of theoretical errors is done. This is very useful and, comparing the results obtained there with those of Ref. [40] using only the lowest order Lagrangian, one can see that the results with the lowest order fall well within the theoretical uncertainties of the higher order calculations.

Two modifications to the above transition amplitudes of Eq. (4) must be introduced to better describe the phase shifts and inelasticities of S_{11} and S_{31} πN scattering. The first modification is due to the realization that the lowest order chiral Lagrangian may be viewed as an effective manifestation of the vector-meson exchange between the mesons and the baryons in an alternative picture, the hidden gauge formalism [41,42], which is shown to be equivalent to the use of chiral Lagrangians [43]. Therefore, to account for the dependence on the momentum transfer of the vector-meson propagator, one replaces C_{ij} with

$$C_{ij}\int\frac{d\hat{k}'}{4\pi}\frac{-m_v^2}{(k'-k)^2 - m_v^2} \tag{5}$$

at

$$\sqrt{s} > \sqrt{s_{ij}^0}, \tag{6}$$

where $\sqrt{s_{ij}^0}$ is the energy where the above integral is unity and which appears between the thresholds of the two i, j channels.

The second modification is the effective inclusion of the $\pi N \to \pi\pi N$ channel. This channel was very important to obtain a good description of the $I = 3/2$ amplitudes but it has only a small influence in the $I = 1/2$ channel [5]. Following Refs. [12] and [44], in the $Q = +1$ sector, this can be achieved by a modification of the potential, i.e., $V_{\pi N\to\pi N} \to V_{\pi N\to\pi N} + \delta V \times G_{\pi\pi N}$, with δV given by

$$\delta V_{\pi^0 p\to\pi^0 p} = \left(-\frac{\sqrt{2}}{3}v_{31} - \frac{1}{3\sqrt{2}}v_{11}\right)^2 + \left(\frac{1}{3}v_{31} - \frac{1}{3}v_{11}\right)^2, \tag{7}$$

$$\delta V_{\pi^0 p\to\pi^+ n} = \left(-\frac{\sqrt{2}}{3}v_{31} - \frac{1}{3\sqrt{2}}v_{11}\right)\left(\frac{1}{3}v_{31} - \frac{1}{3}v_{11}\right) + \left(\frac{1}{3}v_{31} - \frac{1}{3}v_{11}\right)\left(-\frac{1}{3\sqrt{2}}v_{31} - \frac{\sqrt{2}}{3}v_{11}\right), \tag{8}$$

$$\delta V_{\pi^+ n\to\pi^+ n} = \left(\frac{1}{3}v_{31} - \frac{1}{3}v_{11}\right)^2 + \left(-\frac{1}{3\sqrt{2}}v_{31} - \frac{\sqrt{2}}{3}v_{11}\right)^2, \tag{9}$$

where $G_{\pi\pi N}$ is the $\pi\pi N$ loop function that incorporates the two-pion relative momentum squared, whose analytic expression together with those of v_{31} and v_{11} can be found in Ref. [5].

Searching for poles in the isospin 1/2 channel on the second Riemann sheet, one finds the $N^*(1535)$ pole at $1543 - i46$ MeV [5], whose width is smaller than the PDG estimation of $100 \sim 250$ MeV but in agreement with the BES $J/\psi \to \bar{p}\eta p$ data, 95 ± 15 MeV [16].

The moduli of the unitarized amplitudes $|T_{ij}|$ with i any of the six coupled channels and j ηp or $K^+\Lambda$ are shown in Fig. 1. It is interesting to note that the amplitude around the $N^*(1535)$ does not behave like an usual Breit-Wigner resonance, even at the peak position. Therefore, a pole simplification of this resonance by

$$T_{ij} = \frac{g_i g_j}{\sqrt{s} - M_{N^*} + i\Gamma/2} \tag{10}$$

might lead to problems. We come back to this issue in Sec. IV.

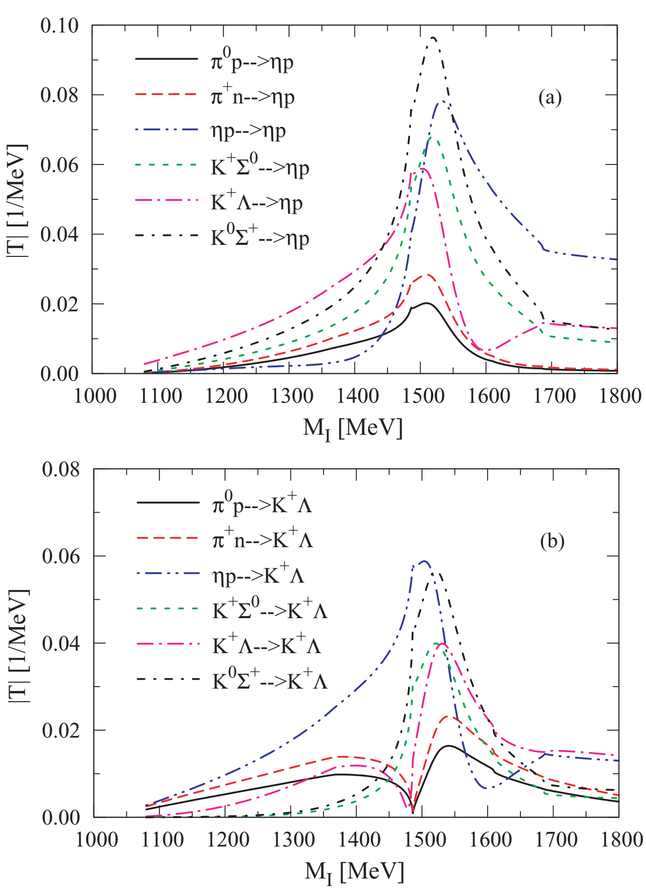

FIG. 1. (Color online) The moduli of the transition amplitudes in different channels leading to the ηp and $K^+\Lambda$ final states.

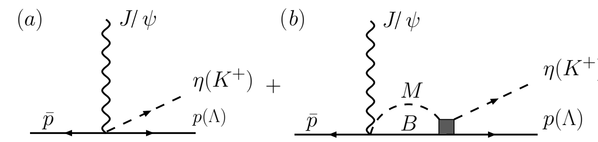

FIG. 2. The reaction mechanisms of $J/\psi \to \bar{p}\eta p$ and $J/\psi \to \bar{p}K^+\Lambda$ through intermediate $N^*(1535)$. For $J/\psi \to \bar{p}p\eta$ a similar diagram through $\bar{N}^*(1535)$ has been added.

III. REACTION MECHANISMS OF $J/\psi \to \bar{p}\eta p$ AND $J/\psi \to \bar{p}K^+\Lambda$

The picture of the $N^*(1535)$ as dynamically generated from the meson-baryon interaction has a repercussion in the mechanisms of production. One must first produce the relevant meson-baryon components, which upon interaction produce the resonance. This means that the J/ψ decaying into $\bar{p}\eta p$ and $\bar{p}K^+\Lambda$ proceeds through the following steps: the J/ψ first decays into $\bar{p}MB$, with MB being one of the six coupled channels. The rescattering of the MB pair generates dynamically the $N^*(1535)$, which then decays back into any of the coupled channels. Such a process is illustrated in Fig. 2.

Because the J/ψ is a SU(3) singlet, its couplings to the $\bar{p}MB$ system can be obtained from the D and F terms of the lowest order chiral Lagrangian of Eq. (3). This SU(3) argument still would have D and F as free parameters in $J/\psi \to \bar{p}\eta p$ ($\bar{p}K^+\Lambda$). However, the $J/\psi \to \bar{P}MB$ process is OZI forbidden (the $c\bar{c}$ quarks of J/ψ decouple from those of the $\bar{p}MB$ system) and it only brings into the scheme a $\vec{\sigma}\cdot\vec{\epsilon}$ operator, which is SU(3) blind. We can then invoke SU(6) symmetry, mixing spin and flavor, to evaluate the $\vec{\sigma}\cdot\vec{\epsilon}$ coupling with two octets of the baryons, with their SU(3) and spin functions, and the octet of the mesons. Assuming this symmetry, the ratio F/D is fixed to the value 2/3 [45], very close to the empirical value. Because we only need the ratio F/D, the SU(6) symmetry provides us with the needed value. Therefore, we take F and D as the empirical values up to a common constant C. The couplings are listed in Table I, where we have assumed C to be 1 because later on we are only interested in the ratio of the integrated cross sections, not their respective absolute values.

The t matrix of the reaction mechanism of Fig. 2 can be easily written down (up to a global $\vec{\sigma}\vec{\epsilon}$ factor with $\vec{\epsilon}$ being the J/ψ polarization vector) as

$$t_i = \sum_{j=1}^{6} D_j(\delta_{ji} + G_j T_{j\to i}), \tag{11}$$

where D_j is the coupling of the J/ψ to channel j (see Table I), G_j the one-baryon one-meson loop function, and $T_{j\to i}$ the unitarized amplitude. The corresponding invariant

TABLE I. The coupling of J/ψ to $\bar{p}MB$ with MB being one of the six coupled channels.

$\pi^0 p$	$\pi^+ n$	ηp	$K^+\Sigma^0$	$K^+\Lambda$	$K^0\Sigma^+$
$\frac{D+F}{2f_\pi}$	$\frac{D+F}{\sqrt{2}f_\pi}$	$\frac{3F-D}{2\sqrt{3}f_\eta}$	$\frac{D-F}{2f_K}$	$-\frac{D+3F}{2\sqrt{3}f_K}$	$\frac{D-F}{\sqrt{2}f_K}$

mass distribution for the $J/\psi \to \bar{p}K^+\Lambda$ reaction is quite simple:

$$\frac{d\Gamma}{dM_I} = \frac{M_{\bar{p}}M_\Lambda}{8\pi^3}\frac{1}{M_{J/\psi}^2}k_{\bar{p}}\tilde{k}_\Lambda|t_5|^2, \tag{12}$$

where

$$k_{\bar{p}} = \frac{\lambda^{1/2}\left(M_{J/\psi}^2, M_{\bar{p}}^2, M_I^2\right)}{2M_{J/\psi}}, \tag{13}$$

$$\tilde{k}_\Lambda = \frac{\lambda^{1/2}\left(M_I^2, m_K^2, M_\Lambda^2\right)}{2M_I} \tag{14}$$

with M_Λ and m_K being the masses of the Λ and kaon, and t_5 given in Eq. (11).

For the reaction $J/\psi \to \bar{p}\eta p$, because it can proceed through either intermediate N^* or intermediate $\bar{N}^*$, one cannot derive such a simple expression. The total width for this reaction is

$$\Gamma = \frac{1}{2M_{J/\psi}}\frac{1}{(2\pi)^5}\frac{M_p^2}{2}\int dE_p\int d\Omega_p\int d\omega_\eta\int d\phi_\eta \times |t_3(N^*) + t_3(\bar{N}^*)|^2\Theta(1-A)^2\Theta(M_{J/\psi} - E_p - \omega_\eta), \tag{15}$$

where M_p, E_p, and Ω_p are the mass, energy, and solid angle of the proton, while ω_η and ϕ_η are the energy of the eta and its azimuthal angle relative to the proton, and A is

$$A = \frac{1}{2k_pk_\eta}\left[(M_{J/\psi} - E_p - \omega_\eta)^2 - M_p^2 - k_p^2 - k_\eta^2\right], \tag{16}$$

with k_p and k_η being the moduli of the three-momenta of the proton and the eta in the J/ψ rest frame.

The amplitude $t_3(\bar{N}^*)$ is the same as that of Eq. (11) for the $p\eta$ amplitude, omitting the δ_{ij} not to double count, but written as a function of the invariant mass of $\bar{p}\eta$ instead of that of $p\eta$. The consideration of $t_3(\bar{N}^*)$ accounts for the final state interaction of $\eta\bar{p}$; however, we should in principle also care about the final state interaction of $K^+\bar{p}$, $\bar{p}p$, or $\bar{p}\Lambda$. The $\eta\bar{p}$ interaction has been singled out because one can have the $\bar{N}^*(1535)$ formation with $\bar{p}\eta$ as well as the $N^*(1535)$ formation with $p\eta$. The interactions of the other pairs are different. The $K^+\bar{p}$ couples strongly to the $\bar{\Lambda}(1405)$. However, this resonance is below the $K^+\bar{p}$ threshold, and we are interested in the region of $K^+\Lambda$ energies around threshold, where the invariant mass of $K^+\bar{p}$ is far away from the $\bar{\Lambda}(1405)$ in the J/Ψ decay, which has 550 MeV of excess energy. However, one spans the region where the $\bar{\Lambda}(1670)$ appears. This resonance appears also as dynamically generated in the chiral approach that we use for the $K^+\bar{p}$ (K^-p) interaction [25], and, because of that, we take this interaction into account. We can use similar arguments for the $\bar{p}p$ and $\bar{p}\Lambda$ interactions, which will have relatively large invariant masses. In these cases the potential energy is small compared to the kinetic energy and accordingly the wave function diverts little from the plane wave, thus barely modifying the production amplitudes [46–48].

IV. RESULTS AND DISCUSSIONS

A. Comparison with the data

The invariant mass distributions for the reactions $J/\psi \to \bar{p}\eta p$ and $J/\psi \to \bar{p}K^+\Lambda$ are shown in Fig. 3. As argued in the previous section, we have used the same D and F coefficients as the couplings of the pseudoscalars to the baryon octet: $D = 0.795$ and $F = 0.465$ [46,49,50]. In the figure, the curves labeled with an "F" are obtained with the full UχPT amplitudes as described above, while the curves labeled with an "S" are obtained with the amplitudes without the $\pi N \to \pi\pi N$ and vertex corrections as explained below. It is seen that the differences between the results obtained with the full amplitudes and those with the amplitudes without the $\pi\pi N$ channel and vertex corrections are rather large beyond ~1650 MeV. This should not worry us much because we are only interested up to this energy. Below this energy, the invariant mass distributions peak at slightly different energies, but this does not change the integrated cross section a lot.

Now we are in a position to compare the theoretical ratio of the two integrated cross sections with the data. However, our model for the dynamical generation of the $N^*(1535)$ is reliable only up to ~1650 MeV. Thus, we can only compare the integrated decay width up to this energy. The experimental ratio is estimated to be

$$R_{\text{exp.}} = \frac{\Gamma(J/\psi \to \bar{p}K^+\Lambda)}{\Gamma(J/\psi \to \bar{p}\eta p)} = \frac{(0.89 \pm 0.16 \times 10^{-3}) \times 10\%}{(2.09 \pm 0.18 \times 10^{-3}) \times 31\%} \approx 0.14 \pm 0.04. \tag{17}$$

The numbers $0.89 \pm 0.16 \times 10^{-3}$ and $2.09 \pm 0.18 \times 10^{-3}$ are the branching ratios for the J/ψ decaying into $\bar{p}K^+\Lambda$ and $\bar{p}\eta p$ [6]. The fraction 10% of the strength of $J/\psi \to \bar{p}K^+\Lambda$ up to $M_I = 1650$ MeV is estimated by studying the $J/\psi \to \bar{p}K^+\Lambda$

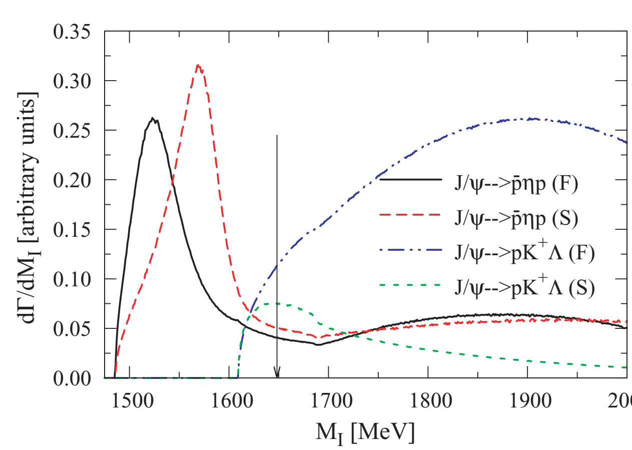

FIG. 3. (Color online) Invariant mass distributions of $J/\psi \to \bar{p}\eta p$ and $J/\psi \to \bar{p}K^+\Lambda$. The theoretical results labeled "F" are obtained using the full UχPT amplitudes containing the vertex and $\pi\pi N$ loop corrections, while the ones labeled "S" are obtained by using the amplitudes without these two corrections and with the readjusted subtraction constants by fitting the $\pi^-p \to KY$ data [14].

experimental spectrum (see Fig. 9b of Ref. [17]). The number 31% is the estimated fraction of the amount of $J/\psi \to \bar{p}\eta p$ up to the same energy (see Fig. 8 of Ref. [16]).

It should be noted that the above ratio has been obtained by using only the raw data to avoid uncertainties related to the further treatments of the data. On the other hand, using the results of the partial wave analyses of Refs. [16] and [17], the ratio is estimated to be

$$R_{\text{exp.}} = \frac{\Gamma(J/\psi \to \bar{p}N^* \to \bar{p}K^+\Lambda)}{\Gamma(J/\psi \to \bar{p}N^* + p\bar{N}^* \to \bar{p}\eta p)} = \frac{(0.89 \pm 0.16 \times 10^{-3}) \times (15 \sim 22)\%}{(2.09 \pm 0.18 \times 10^{-3}) \times (56 \pm 15)\%} \approx 0.14^{+0.15}_{-0.07}, \tag{18}$$

which is the ratio fitted to obtain the $N^*(1535)$ coupling constant to $K\Lambda$ in Ref. [7]. We note that the ratios obtained either way are consistent with each other, albeit with large uncertainties.

On the other hand, our theoretical ratio of the integrated cross sections from the respective thresholds up to $M_I = 1650$ MeV (using the full amplitudes) is

$$R_{\text{th}} = \frac{\Gamma(J/\psi \to \bar{p}N^* \to \bar{p}K^+\Lambda)}{\Gamma(J/\psi \to \bar{p}N^* + p\bar{N}^* \to \bar{p}\eta p)} = 0.16^{+0.06}_{-0.04}, \tag{19}$$

which is in reasonable agreement with the experimental ratio determined either way. The theoretical uncertainties are estimated by slightly changing the F/D ratio appearing in the J/ψ couplings to $\bar{p}MB$ by 5%.

It is interesting to note that the theoretical ratio is obtained by assuming SU(6) symmetry for the J/ψ to $\bar{p}MB$ couplings and by assuming, for the reasons given above, that the D and F coefficients are the same as those appearing in the Yukawa couplings of one pseudoscalar to the octet of baryons, up to a global constant. The agreement with the data supports these assumptions.

Another source of inherent theoretical uncertainties comes from the consideration of the $\pi\pi N$ channel, the vertex correction, and the freedom one has in the values of the subtraction constants. Following Ref. [14], we assess these uncertainties by removing the contribution of the $\pi\pi N$ channel and the vertex corrections and adjusting the subtraction constants to fit the $\pi^- p \to KY$ cross-section data at higher energies. The corresponding invariant mass distributions obtained this way are shown in Fig. 3, the curves labeled with an "S". It is seen that the ηp peak position is moved to slightly higher energies by ∼30 MeV, while the ratio of the two integrated cross sections is reduced to ∼0.11. Combining the results with the full and the "simplified" UχPT amplitudes, we arrive at the theoretical ratio

$$R_{\text{th}} = 0.135 \pm 0.06, \tag{20}$$

where the central value is an average of the ratios obtained with the full amplitudes and the simplified amplitudes and the dispersion incorporates both the uncertainties in the UχPT amplitudes and those in the D and F coefficients.

Above we have shown that the two experimental ratios Eq. (17) and Eq. (18) are consistent with each other. However, there is a caveat in our comparison with these two numbers.

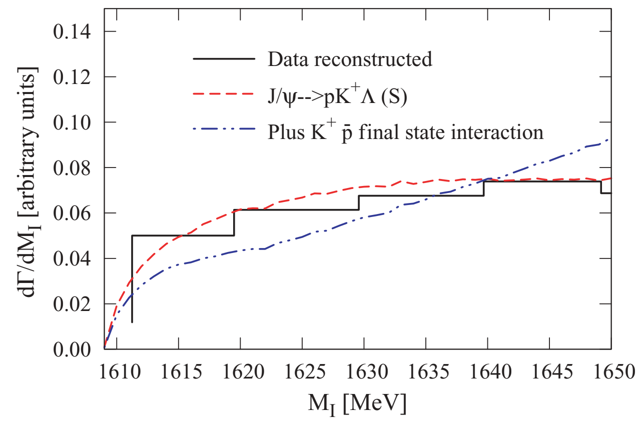

FIG. 4. (Color online) The invariant mass distributions of the $J/\psi \to \bar{p}K^+\Lambda$ reaction with and without the $K^+\bar{p}$ final state interaction [40].

Our above comparison with the experimental ratio of Eq. (18) is fine, because this ratio is obtained solely from N^* contributions as explained by the corresponding experimental analysis. Our comparison with the experimental ratio of Eq. (17), on the other hand, is not very consistent because in this case we have to include the $K^+\bar{p}$ final state interaction in the same way we included the $\eta\bar{p}$ interaction. The $K^+\bar{p}$ interaction has been studied extensively in unitary chiral theories and is well understood around the $K^+\bar{p}$ threshold and, to a lesser degree, around the $\bar{\Lambda}(1670)$ peak position. For energies beyond the $\bar{\Lambda}(1670)$ peak position, it is less constrained and the comparison with data is only qualitative [25]. Despite all the uncertainties of the $K^+\bar{p}$ interaction, it is still interesting to see how adding this part will change the scenario. Following a procedure similar to that of including the $\eta\bar{p}$ contribution and using the same argument to obtain the couplings of the J/ψ to the ten channels coupling to $K^+\bar{p}$, we find that adding the $K^+\bar{p}$ final state interaction only changes our calculated ratio by ∼10% percent, which is smaller than the theoretical errors. The corresponding invariant mass distributions are shown in Fig. 4, in comparison with the results obtained without including the $K^+\bar{p}$ final state interaction—the curve denoted by (S) in Fig. 3. The experimental numbers are obtained by multiplying by phase space the numbers shown in Fig. 9 of Ref. [17].

We can conclude from the above discussion that the theoretical ratio is rather stable despite the relatively large uncertainties of the $K^+\bar{p}$ final state interaction. This is true partly because we confine ourselves to $K^+\Lambda$ center of mass energies below ∼1650 MeV where the $K^+\bar{p}$ interaction is relatively well constrained due to the three-body phase space.

B. Couplings constants in different models

It is instructive to compare the ratio of the $N^*(1535)$ effective couplings obtained in the unitary chiral approach of Ref. [5] and that obtained in Ref. [7], because both models describe the J/ψ decay data. Using the numbers from Ref. [5], one has $|g_{N^*(1535)K\Lambda}| = 0.92$ and $|g_{N^*(1535)\eta N}| = 1.84$

obtained from the residues of the T amplitudes at the pole position on the complex plane. On the other hand, from the same study, one finds $|g_{N^*(1535)K\Lambda}| = 1.28$ and $|g_{N^*(1535)\eta N}| = 1.77$ through a Breit-Wigner fit of the real energy scattering amplitudes. Thus, we obtain

$$R = \frac{|g_{N^*(1535)K\Lambda}|}{|g_{N^*(1535)\eta N}|} = 0.5 \sim 0.7. \tag{21}$$

This is a factor of two smaller than the one obtained in Ref. [7], 1.3 ± 0.3, from the comparative study of the reactions studied in the present work, and is slightly smaller than the range of $0.8 \sim 2.6$ given in Ref. [51].

The relatively large discrepancy between the phenomenologically determined R and the UχPT ones reveals a fundamental difference in these two different descriptions of resonances, particularly in the region far from the resonance peak position, which is relevant to the present study. In the phenomenological description one often adopts a Breit-Wigner-like formula to describe the distribution of a resonance,

$$\frac{\tilde{g}_i \tilde{g}_j}{(S - M^2) + i M \Gamma(s)}, \tag{22}$$

where $\tilde{g}_i$, $\tilde{g}_j$ are the coupling constants of the resonance to channels i and j, M is the mass of the resonance, and $\Gamma(s)$ is the width of the resonance, which incorporates the explicit energy dependence. This is the type of amplitudes used in Ref. [7] to describe the J/ψ decay processes.

This approximation assumes that the resonance's shape in different channels is the same, while the only difference comes from the coupling constants. This could be a valid approximation in many cases, but it is not true in the present case, as can be clearly seen from Fig. 1. There, one can easily see that even around the resonance peak position the shapes in different channels are not proportional to each other. The deviations become even larger at the $K^+\Lambda$ threshold. The dynamics of coupled channels is mostly responsible for that [2–5], and particularly the large coupling of the resonance to the ηN channel close to threshold. This particular behavior of the resonance might explain the relatively large discrepancy between the coupling constants obtained in different methods, though they both describe the data.

One may well conclude that the coupling constants determined from chiral unitary theory and those determined from phenomenological studies cannot be directly compared: They only have meanings inside the framework where they are deduced, at least quantitatively. This has also been pointed out recently in Ref. [14].

Of course, one of the aims of the present work is to show consistency of the present two J/ψ decay reactions with the idea of the $N^*(1535)$ resonance as being dynamically generated in the chiral unitary approach, and we see that indeed the UχPT picture is consistent with the BES data. Note that we have not fitted the experimental data to obtain the $N^*\Lambda K$ couplings, as is the case in Ref. [7]. We have used the results of Ref. [5] in the context of the two J/ψ reactions and have found consistency with the data, with some uncertainties tied to the nature of these two reactions beyond the dynamics of the meson-baryon interaction, as we have explained above. We found consistency with the data even if the UχPT picture produces a coupling for $N^*K\Lambda$ different than that in Ref. [7], but we also have mentioned that the meaning of the couplings is not exactly the same because of the different shapes used for the energy dependence of the amplitudes. Furthermore, the approach followed here does not make any explicit use of the $g_{N^*(1535)K\Lambda}$ coupling because we used the full MB amplitudes. These amplitudes are different from the simple pole approximation that one would obtain extrapolating the form of Eq. (22) with constant Γ to higher energies.

A further remark concerning the meaning of the couplings: The one obtained in Ref. [5] comes from the residue of the N^* pole, while the one from Ref. [7] comes from fits to data around the $K\Lambda$ threshold. The former is a measure of the strength of the $K\Lambda$ component in the $N^*(1535)$ wave function and plays a role in the determination of the properties of the $N^*(1535)$. For instance, if one wishes to determine the helicity amplitudes of the $N^*(1535)$ as done in Ref. [13], it is the residue of the N^* pole that must be used in the calculation.

V. SUMMARY

We have studied the $J/\psi \to \bar{p}\eta p$ and $J/\psi \to \bar{p}K^+\Lambda$ reactions, more specifically, the ratio of the integrated cross sections, using the unitary chiral approach. The unitary chiral approach, which generates the $N^*(1535)$ dynamically, can describe the data reasonably well. This was despite the fact that the coupling of the $N^*(1535)$ to the $K\Lambda$ channel is different from the one obtained in the empirical study of the present reactions in Ref. [7], but it was clarified that the concepts are different. The couplings of the chiral unitary approach come from the residues of the amplitudes at the N^* pole, while the $N^*\Lambda K$ coupling obtained in Ref. [7] comes from a fit to the data close to the $K\Lambda$ threshold assuming a certain shape for the N^* dominated amplitude. Furthermore, it is interesting to note that although the couplings obtained in different ways are quantitatively different, they both indicate that the $N^*(1535)$ wave function contains a large $s\bar{s}$ component.

Certainly, the $N^*(1535)$ may in fact be a mixture of a three-quark component and a five-quark (meson-baryon) component, as suggested by the studies of Ref. [52]. This may slightly change the numbers obtained in this work, but the main conclusions, taking into account both theoretical and experimental uncertainties, will remain the same.

ACKNOWLEDGMENTS

We would like to thank Pedro Gonzalez for useful discussions. This work is partly supported by FIS2006-03438, by the National Natural Science Foundation of China and the Chinese Academy of Sciences under Project KJCX3-SYW-N2, by the Generalitat Valenciana, and by the EU Integrated Infrastructure Initiative Hadron Physics Project under Contract RII3-CT-2004-506078.

[1] S. Capstick and W. Roberts, Prog. Part. Nucl. Phys. **45**, S241 (2000).
[2] N. Kaiser, P. B. Siegel, and W. Weise, Phys. Lett. **B362**, 23 (1995).
[3] N. Kaiser, T. Waas, and W. Weise, Nucl. Phys. **A612**, 297 (1997).
[4] J. Nieves and E. R. Arriola, Phys. Rev. D **64**, 116008 (2001).
[5] T. Inoue, E. Oset, and M. J. Vicente Vacas, Phys. Rev. C **65**, 035204 (2002).
[6] W. M. Yao *et al.* (Particle Data Group), J. Phys. G **33**, 1 (2006).
[7] B. C. Liu and B. S. Zou, Phys. Rev. Lett. **96**, 042002 (2006).
[8] B. C. Liu and B. S. Zou, Phys. Rev. Lett. **98**, 039102 (2007).
[9] B.-C. Liu and B.-S. Zou, Commun. Theor. Phys. **46**, 501 (2006).
[10] V. Shklyar, H. Lenske, and U. Mosel, Phys. Rev. C **72**, 015210 (2005).
[11] B. Julia-Diaz, B. Saghai, T. S. H. Lee, and F. Tabakin, Phys. Rev. C **73**, 055204 (2006).
[12] M. Döring, E. Oset, and D. Strottman, Phys. Rev. C **73**, 045209 (2006).
[13] D. Jido, M. Döring, and E. Oset, Phys. Rev. C **77**, 065207 (2008).
[14] M. Döring, E. Oset, and B. S. Zou, Phys. Rev. C **78**, 025207 (2008).
[15] B.-S. Zou, Nucl. Phys. **A684**, 330 (2001).
[16] J. Z. Bai *et al.* (BES Collaboration), Phys. Lett. **B510**, 75 (2001).
[17] H.-X. Yang (BES Collaboration), Int. J. Mod. Phys. A **20**, 1985 (2005).
[18] J. T. Balewski *et al.*, Phys. Lett. **B420**, 211 (1998).
[19] R. Bilger *et al.*, Phys. Lett. **B420**, 217 (1998).
[20] S. Sewerin *et al.*, Phys. Rev. Lett. **83**, 682 (1999).
[21] P. Kowina *et al.*, Eur. Phys. J. A **22**, 293 (2004).
[22] J. A. Oller and E. Oset, Nucl. Phys. **A620**, 438 (1997).
[23] T. S. H. Lee, J. A. Oller, E. Oset, and A. Ramos, Nucl. Phys. **A643**, 402 (1998).
[24] T. Hyodo, S. I. Nam, D. Jido, and A. Hosaka, Phys. Rev. C **68**, 018201 (2003).
[25] E. Oset, A. Ramos, and C. Bennhold, Phys. Lett. **B527**, 99 (2002).
[26] B. Borasoy, R. Nissler, and W. Weise, Eur. Phys. J. A **25**, 79 (2005).
[27] J. A. Oller, M. Verbeni, and J. Prades, J. High Energy Phys. 09 (2006) 079.
[28] B. Borasoy and R. Nissler, Eur. Phys. J. A **26**, 383 (2005).
[29] B. Borasoy, U. G. Meissner, and R. Nissler, Phys. Rev. C **74**, 055201 (2006).
[30] T. N. Truong, Phys. Rev. Lett. **61**, 2526 (1988).
[31] F. Guerrero and J. A. Oller, Nucl. Phys. **B537**, 459 (1999).
[32] J. R. Pelaez, Mod. Phys. Lett. A **19**, 2879 (2004).
[33] J. A. Oller and E. Oset, Phys. Rev. D **60**, 074023 (1999).
[34] J. A. Oller and U. G. Meissner, Phys. Lett. **B500**, 263 (2001).
[35] E. E. Salpeter and H. A. Bethe, Phys. Rev. **84**, 1232 (1951).
[36] A. D. Lahiff and I. R. Afnan, Phys. Rev. C **60**, 024608 (1999).
[37] E. Oset *et al.*, Pramana **66**, 731 (2006).
[38] M. Döring, E. Oset, and S. Sarkar, Phys. Rev. C **74**, 065204 (2006).
[39] V. Bernard, N. Kaiser, and U.-G. Meissner, Int. J. Mod. Phys. E **4**, 193 (1995).
[40] E. Oset and A. Ramos, Nucl. Phys. **A635**, 99 (1998).
[41] M. Bando, T. Kugo, S. Uehara, K. Yamawaki, and T. Yanagida, Phys. Rev. Lett. **54**, 1215 (1985).
[42] M. Bando, T. Kugo, and K. Yamawaki, Phys. Rep. **164**, 217 (1988).
[43] G. Ecker, J. Gasser, H. Leutwyler, A. Pich, and E. de Rafael, Phys. Lett. **B223**, 425 (1989).
[44] M. Döring, E. Oset, and M. J. Vicente Vacas, Phys. Rev. C **70**, 045203 (2004).
[45] F. Gürsey, A. Pais, and L. A. Radicati, Phys. Rev. Lett. **13**, 299 (1964).
[46] M. Goldberger and K. Watson, *Collision Theory* (Wiley, New York, 1964).
[47] K. M. Watson, Phys. Rev. **88**, 1163 (1952).
[48] C. Hanhart, Phys. Rep. **397**, 155 (2004).
[49] F. E. Close and R. G. Roberts, Phys. Lett. **B316**, 165 (1993).
[50] B. Borasoy, P. C. Bruns, U.-G. Meissner, and R. Nissler, Eur. Phys. J. A **34**, 161 (2007).
[51] G. Penner and U. Mosel, Phys. Rev. C **66**, 055212 (2002).
[52] T. Hyodo, D. Jido, and A. Hosaka, Phys. Rev. C **78**, 025203 (2008).